



U.S. DEPARTMENT OF
ENERGY

PNNL-22185

Prepared for the U.S. Department of Energy
under Contract DE-AC05-76RL01830

Modeling the Air Flow in the 3410 Building Filtered Exhaust Stack System

KP Recknagle
SR Suffield

JM Barnett

January 2013



Pacific Northwest
NATIONAL LABORATORY

*Proudly Operated by **Battelle** Since 1965*

DISCLAIMER

This report was prepared as an account of work sponsored by an agency of the United States Government. Neither the United States Government nor any agency thereof, nor Battelle Memorial Institute, nor any of their employees, makes **any warranty, express or implied, or assumes any legal liability or responsibility for the accuracy, completeness, or usefulness of any information, apparatus, product, or process disclosed, or represents that its use would not infringe privately owned rights.** Reference herein to any specific commercial product, process, or service by trade name, trademark, manufacturer, or otherwise does not necessarily constitute or imply its endorsement, recommendation, or favoring by the United States Government or any agency thereof, or Battelle Memorial Institute. The views and opinions of authors expressed herein do not necessarily state or reflect those of the United States Government or any agency thereof.

PACIFIC NORTHWEST NATIONAL LABORATORY

operated by

BATTELLE

for the

UNITED STATES DEPARTMENT OF ENERGY

under Contract DE-AC05-76RL01830

Printed in the United States of America

Available to DOE and DOE contractors from the
Office of Scientific and Technical Information,
P.O. Box 62, Oak Ridge, TN 37831-0062;
ph: (865) 576-8401
fax: (865) 576-5728
email: reports@adonis.osti.gov

Available to the public from the National Technical Information Service,
U.S. Department of Commerce, 5285 Port Royal Rd., Springfield, VA 22161
ph: (800) 553-6847
fax: (703) 605-6900
email: orders@ntis.fedworld.gov
online ordering: <http://www.ntis.gov/ordering.htm>



This document was printed on recycled paper.

(9/2003)

Modeling the Air Flow in the 3410 Building Filtered Exhaust Stack System

KP Recknagle
SR Suffield

JM Barnett

January 2013

Prepared for
the U.S. Department of Energy
under Contract DE-AC05-76RL01830

Pacific Northwest National Laboratory
Richland, Washington 99352

Executive Summary

Additional ventilation capacity has been designed for the 3410 Building filtered exhaust stack system. The updated system will increase the number of fans from two to three and will include ductwork to incorporate the new fan into the existing stack. Stack operations will involve running various two-fan combinations at any given time. The air monitoring system of the existing two-fan stack was previously found to be in compliance with the ANSI/HPS N13.1-1999 standard, however it is not known if the modified (three-fan) system will comply. Subsequently, a full scale three dimensional (3-D) computational fluid dynamics (CFD) model of the modified stack system has been created to examine the sampling location for compliance with the standard.

The CFD modeling results show good agreement with testing data collected from the existing 3410 Building stack and suggest that velocity uniformity and flow angles will remain well within acceptance criteria when the third fan and associated ductwork is installed. This includes two-fan flow rates up to 31,840 cfm for any of the two-fan combinations. For simulation cases in which tracer gas and particles are introduced in the main duct, the model predicts that both particle and tracer gas coefficients of variance (COVs) may be larger than the acceptable 20 percent criterion of the ANSI/HPS N13.1-1999 standard for each of the two-fan, 31,840 cfm combinations. Simulations in which the tracers are introduced near the fans result in improved, though marginally acceptable, COV values for the tracers.

Due to the remaining uncertainty that the stack will qualify with the addition of the third fan and high flow rates, a stationary air blender from Blender Products, Inc. is considered for inclusion in the stack system. A model of the air blender has been developed and incorporated into the CFD model. Simulation results from the CFD model that includes the air blender show striking improvements in tracer gas mixing and tracer particle dispersion. The results of these simulations suggest the air blender should be included in the stack system to ensure qualification of the stack.

Acronyms and Abbreviations

3-D	three-dimensional
ANSI	American National Standards Institute
HPS	Health Physics Society
CFD	computational fluid dynamics
COV	coefficient of variance
PNNL	Pacific Northwest National Laboratory

Contents

Executive Summary	iii
Acronyms and Abbreviations.....	v
1.0 Introduction.....	1.1
2.0 Modeling Approach.....	2.1
2.1 Flow Model	2.1
2.2 Tracer Gas Model.....	2.2
2.3 Oil Droplet Model	2.2
2.4 Model Geometry	2.2
2.5 Boundary Conditions.....	2.4
3.0 Stack Model Validation	3.1
4.0 Stack Modeling Results	4.1
4.1 Flow Angle and Velocity Uniformity	4.1
4.2 Particle and Tracer Gas Distributions (mid-duct release location)	4.2
4.3 Particle and Tracer Gas Distributions	4.4
4.4 Duct with Air Blender	4.5
5.0 Conclusions.....	5.1
6.0 References.....	6.1

Figures

Figure 2.1. Model Geometry for the Modified 3410 Building Filtered Exhaust Stack System	2.3
Figure 2.2. Detail of Computational Mesh at the (a) Surface Mesh Near Fan 1, and (b) Typical Cross-Section of the Volume Mesh in the Main Duct.....	2.3
Figure 3.1. Velocity Magnitude at the Sampling Section for the Modeled (a) VT-4, and (b) VT-3 Test Cases	3.2
Figure 3.2. Velocity Magnitude in Plan View at Mid-Plane of the Main Duct for the Modeled VT-4 Flow Case.....	3.2
Figure 4.1. Velocity Magnitude at the Sampling Section for the Modeled Flow Rate of 31,840 cfm, Running (a) Fans 1 and 2, (b) Fans 1 and 3, and (c) Fans 2 and 3	4.1
Figure 4.2. Particle Distributions at the Sampling Section for a Total Modeled Flow Rate of 31,840 cfm, Running (a) Fans 1 and 2, (b) Fans 1 and 3, and (c) Fans 2 and 3	4.3
Figure 4.3. Tracer Gas Concentration Contours at the Sampling Section for a Total Modeled Flow Rate of 31,840 cfm, Running (a) Fans 1 and 2, (b) Fans 1 and 3, and (c) Fans 2 and 3.....	4.3
Figure 4.4. Static Air Blender S40C3S: (a) Photograph of Sample Device, (b) CFD Model	4.5
Figure 4.5. Contours of Velocity Magnitude in the Plan View for (a) the Duct with the Air Blender Installed, and (b) No Air Blender.....	4.6
Figure 4.6. Contours of SF6 Tracer Gas Concentration in Plan View for the Duct with (a) the Air Blender Installed, and (b) No Air Blender.....	4.7
Figure 4.7. Tracer Particle Paths Through the Air Blender: (a) 3-D View, and (b) Plan View.....	4.8
Figure 4.8. Tracer Particle Distributions at Several Stations Downstream of the Air Blender	4.9
Figure 4.9. Maximum Flow Angle (degrees) and COV for Velocity, Tracer Gas, and Tracer Particles with Air Blender.....	4.9

Tables

Table 3.1. COV for Velocity Uniformity Tests VT-3 and VT-4	3.3
Table 3.2. Maximum Flow Angles from Tests and Models	3.3
Table 4.1. COV for Velocity Uniformity and Maximum Flow Angles From CFD Modeling.....	4.2
Table 4.2. COV for Particle and Tracer Gas Distributions at the Sampling Section.....	4.3
Table 4.3. COV for Velocity, Particle, and Tracer Distributions at the Sampling Section	4.4

1.0 Introduction

The 3410 Building at Pacific Northwest National Laboratory (PNNL) houses PNNL radiological capabilities. As such, air discharged from the building filtered exhaust stack system must be monitored for radionuclides. The air monitoring system must comply with applicable federal regulations, which subsequently require a sampling probe in the exhaust stream to conform to the uniformity criteria of the ANSI/HPS N13.1-1999 standard. The criteria include the uniformity of flow velocity, the average angle between the flow and duct axis, the uniformity of tracer gas, and the uniformity of tracer particles. The uniformity is expressed by the coefficient of variance (COV), defined as the standard deviation divided by the mean. For a sampling location to be acceptable, COVs for velocity, tracer gas concentration, and tracer particle concentration must be less than 20 percent. Additionally, the average flow angle must be less than 20 degrees from the duct axis (aligned with the sample probe) to ensure the flow is not cyclonic. The standard requires that testing be performed to demonstrate the compliance of the duct and sampling probe for meeting these uniformity criteria.

An option in the ANSI/HPS N13.1-1999 standard allows the adoption of results from a previously performed full test series for a stack system of similar configuration as the basis of compliance with the standard. Compliance is then confirmed by partial testing performed on the actual stack system. This approach was used to qualify the location of the monitoring probe and configuration of the original two-fan 3410 Building filtered exhaust stack, as documented by Glissmeyer and Flaherty in 2010 (PNNL-19562). This testing performed on the actual system included flow velocity uniformity and flow angle measurements. The previous full test series applied as the basis for compliance was that performed on a scale model of the Waste Treatment Plant's HV-C2 air exhaust stack by Glissmeyer and Droppo in 2007 (PNNL-16611). The HV-C2 stack, with two fans entering a horizontal main duct, both at 45 degree angles, is very similar to the original two-fan configuration of the 3410 Building exhaust stack.

The original testing of the HV-C2 scale model (PNNL-16611) was performed to establish the sampling probe location for the actual HV-C2 stack. The scale model showed good velocity uniformity and small flow angles. However, tracer gas/particle test COV values were greater than 20 percent at all but the test port furthest downstream. This furthest test port on the HV-C2 scale model is similar in scaled distance to that of the 3410 Building sampling location. Thus, in the two-fan stack configuration, all of the main duct length of the 3410 Building exhaust system will be needed to provide sufficient mixing of tracer gas and tracer particles.

The 3410 Building exhaust stack system will be updated with additional ventilation capacity. The updated system will incorporate a third fan and adjoining ductwork to integrate the new fan into the existing stack. As a result, the stack configuration will be changed substantially. The normal operating condition will have two fans operating with one fan in standby. The average overall flow rate will also be increased significantly. In the absence of data from a similar system, it is not well known if the updated three-fan system will qualify as readily as the two-fan system. Testing will ultimately be required to prove the stack system and sampling location comply with the ANSI/HPS N13.1-1999 standard. Before making a final decision on installation of the proposed design, modeling would be used to gain more insight into the expected performance of the modified stack.

2.0 Modeling Approach

The purpose of modeling the 3410 Building stack system is to simulate the stack flow, including the distributions of gas and particle tracers, to assist in determining if the modified system will satisfy the ANSI/HPS N13.1-1999 standard. To provide accurate predictions of flow, tracer gas, and tracer particle distributions (at the sampling location) requires an accurate prediction of the turbulent air flow with mixing and transport of the tracer species within it. The geometry and flow field of the exhaust stack system is complex and highly three-dimensional (3-D). Therefore, a representative boundary-fitted, 3-D flow model is also required. The commercially available, computational fluid dynamics (CFD) flow simulation code, STAR-CCM+ (CD-Adapco 2012) was selected for creation of the model geometry and the flow simulations.

2.1 Flow Model

The stack sampling methodology assumes isothermal conditions exist within the stack, thus this assumption is adopted in the flow model. For the isothermal flow solutions, STAR-CCM+ solves the Navier-Stokes conservation of mass and momentum equations, which for steady state compressible and incompressible fluid flows are

$$\frac{\partial}{\partial x_j}(\rho u_j) = 0 \quad (1)$$

$$\frac{\partial}{\partial x_j}(\rho u_j u_i - \tau_{ij}) = -\frac{\partial p}{\partial x_i} \quad (2)$$

where the u_i are the absolute fluid velocity components in coordinate directions x_i ($i = 1, 2, 3$), ρ is the density, p is the pressure, and τ_{ij} is the fluid stress tensor, which for turbulent flows is represented by

$$\tau_{ij} = 2\mu\sigma_{ij} - \frac{2}{3}\mu\frac{\partial u_k}{\partial x_k}\delta_{ij} - \overline{\rho u'_i u'_j} \quad (3)$$

Here μ is the dynamic viscosity, σ_{ij} is the rate of strain tensor, δ_{ij} is the kronecker delta, u_i and u_j are fluctuations about the average velocity, and the overbar indicates the averaging of the fluctuations. The right-most term in equation 3 represents the additional Reynolds stresses due to turbulent motion. These are linked to the mean velocity via the turbulence model being used. In the simulations for this work, the generation and dissipation of turbulence is accounted for using the standard κ - ϵ turbulence model for large Reynolds number flow, as described in the STAR-CMM+ User Guide (CD-Adapco 2012). In past work by Recknagle et al. (2009), a turbulence model comparison found the large Reynolds number κ - ϵ model to be the most suitable for use in simulating duct flow, a finding corroborated by Jenson (2007).

2.2 Tracer Gas Model

For the SF6 tracer gas simulations, the model assumes each species k of a fluid mixture, with local mass fraction Y_k governed by a species conservation equation of the form:

$$\frac{\partial}{\partial x_j} (\rho u_j Y_k + F_{k,j}) = S_k \quad (4)$$

where $F_{k,j}$ is the gas diffusional flux component and S_k is the gas species source term at the injection location.

2.3 Oil Droplet Model

A Lagrangian dispersed two-phase flow model is used for the oil droplet transport simulations. The Lagrangian methodology considers the interactions of mass, momentum, and energy between the continuum and dispersed phases. In general, motion of the dispersed phase is influenced by that of the continuous phase and vice versa. The strength of the phase interactions depend on the dispersed particle's size, density, and number density. For the present work, droplet concentrations are small, as is the nominal particle size, thus momentum transfer from droplets to air is negligibly small. In the model, the momentum equation for a droplet, given by Newton's second law, is

$$m_d \frac{du_d}{dt} = F_{dr} + F_p + F_b \quad (5)$$

where m_d and u_d are the mass and velocity of the dispersed droplet phase, F_{dr} is the drag force, F_p the pressure force, and F_b is body forces including effect of the gravity and angular velocity vectors. Surface vapor pressure and mass transfer between phases is not considered here. The problem is considered isothermal and does not involve electrically charged flow, therefore thermophoresis and electrostatic effects are not included. Because of the low number density of the oil droplets, separation and coalescence models are left aside as well.

2.4 Model Geometry

A design drawing of the 3410 Building exhaust stack system was used to create a 3-D geometry model of the modified stack system. The model geometry for the system is shown in Figure 2.1. Air mixing upstream of the fans is not included in the models. Instead, the model domains include the ductwork from just downstream of the fans to the stack exit. The centerlines of fans 1 and 2 are located above the duct centerline. This geometric feature and the circumferential rotation of the fan blades result in a velocity profile weighted heavily toward the bottom of the duct. To approximate the circumferential motion created by the fans, curved duct segments are included in the model geometry, as shown in the figure. Fan 3 is located below the duct centerline, thus the curved duct section for it is oriented opposite of fans 1 and 2.

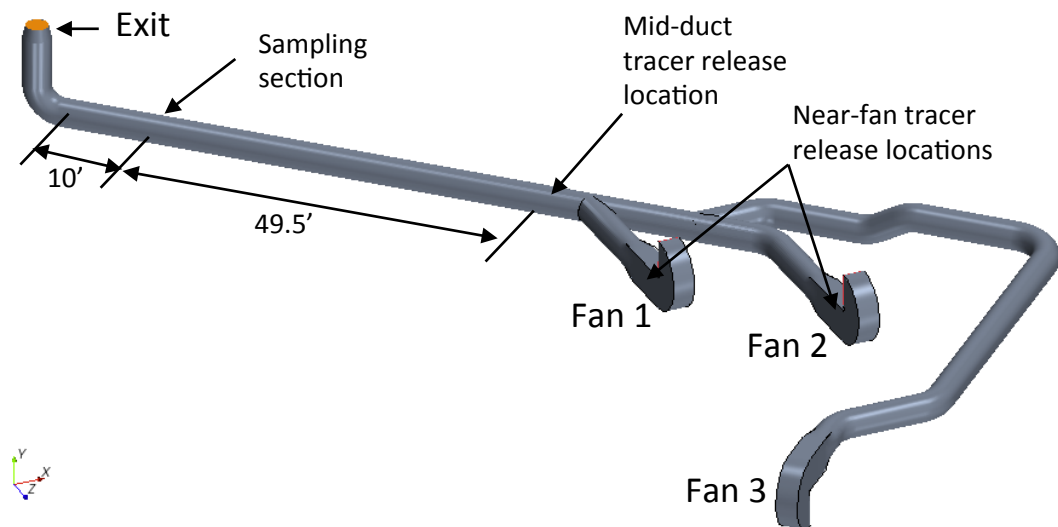


Figure 2.1. Model Geometry for the Modified 3410 Building Filtered Exhaust Stack System

The overall computational mesh is sufficiently refined to enable resolution of the turbulent flow field throughout the system. The computational mesh used for the simulations was developed in a process that tested the solution sensitivity for several mesh resolutions. The final computational mesh for the three-fan system contains 913,628 elements; Figure 2.2a provides a close up view of the mesh near fan 1, including a rectangular extension of the fan inflow boundary that helps establish flow solution stability. Resolution throughout the volume mesh is similar to that shown in Figure 2.2b.

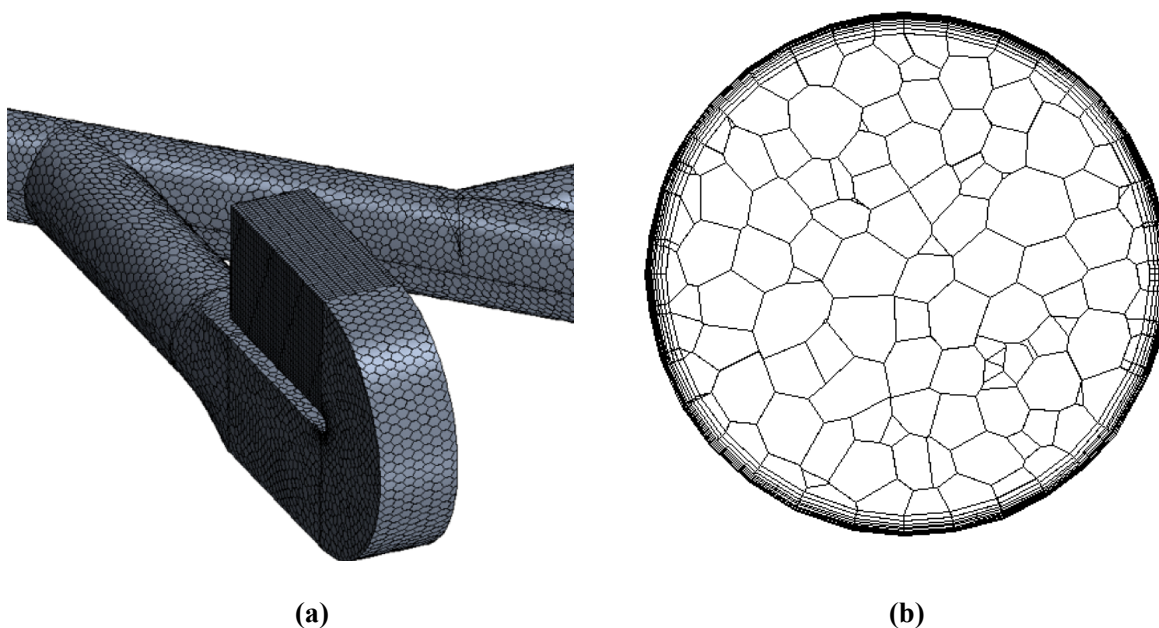


Figure 2.2. Detail of Computational Mesh at the (a) Surface Mesh Near Fan 1, and (b) Typical Cross-Section of the Volume Mesh in the Main Duct

2.5 Boundary Conditions

Mass inflow boundaries with uniform velocity distributions are established at the duct inlets, including turbulence intensity and turbulent viscosity ratio settings. A pressure boundary with 1 atmosphere absolute pressure is used at the stack exit. Duct walls are modeled as smooth surfaces with zero slip flow boundary conditions. The particle boundary condition at the walls is established such that particles with trajectories that intersect with duct walls will bounce from the surface.

3.0 Stack Model Validation

The first simulation cases presented are to validate the capability of the model to replicate flow angle and velocity uniformity measurements taken from the actual 3410 Building stack. As validation, the modeled flow uniformity, as indicated by the COV of velocity uniformity at the side and top sampling ports, is compared to measured data. Per the design drawing of the 3410 Building exhaust stack system, the top and side sampling ports are located 10 feet, 0 inches upstream of the 90-degree elbow near the stack exit, as shown in Figure 2.1. This is the location used in the model to extract velocity information for comparison with the measured data. This location is 49.5 feet (or 15 duct diameters) downstream of main-duct release location near the junction of fan 1 with the main duct.

A substantial length of duct is required to achieve a fully developed velocity profile (fully developed flow). For turbulent flow, this hydrodynamic flow development length (x_{fd}) is considered to be roughly independent of the Reynolds number, ranges from 10- to 60-diameters, and is typically assumed to be at least 10-diameters (Incropera and DeWitt 1985). A more conservative relation for x_{fd} (Young, Munson, and Okiishi 1997) considers the Reynolds number dependence, such that

$$\frac{x_{fd}}{D} = 4.4 (Re)^{1/6} \quad (6)$$

Using this expression, x_{fd} would range from 37-diameters for a flow (in the 40-inch duct) of 10,000 cfm, to 45-diameters for a flow of 31,840 cfm (two fans operating at 15,920 cfm). With this Reynolds number dependence in mind, and the actual length available in the duct for flow development, we sought to gain validation of the model from measured data from a range of flow cases. Glissmeyer and Flaherty (PNNL-19562) measured velocity profiles for flows of 20,450 and 12,351 acfm, in tests VT-3 and VT-4, respectively. Simulation cases using the full-scale CFD model of the existing system were run to replicate the conditions tested in VT-3 and VT-4.

Figure 3.1 shows the modeled velocity magnitude profile at the sampling section for (a) VT-4 and (b) VT-3. The location of maximum velocity, skewed low and to the left of center, is similar for both flow rate cases. The skewed flow at the sampling location is due to a slight swirling effect in the main duct setup by the circumferential flow introduced by fans 1 and 2, and the confluence of the two streams into the main duct. This effect can be seen in plan view in Figure 3.2, which shows the velocity magnitude at the mid-plane of the main duct as the flow swirls in a counter clock-wise direction, making about two-thirds of a full rotation along the duct. The location of the sampling section is indicated in Figure 3.2 by the vertical line through the duct at left.

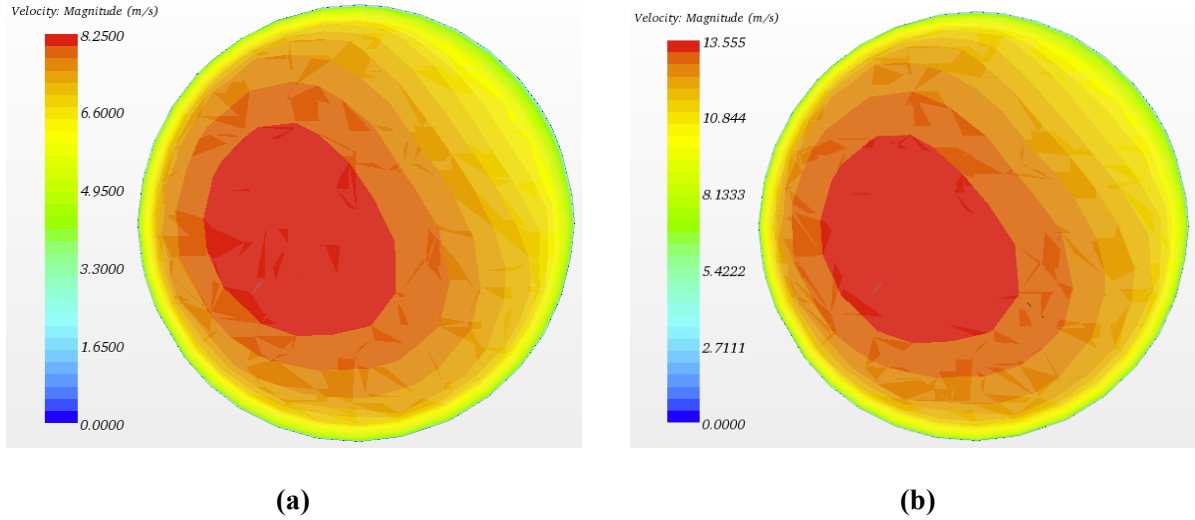


Figure 3.1. Velocity Magnitude at the Sampling Section for the Modeled (a) VT-4, and (b) VT-3 Test Cases

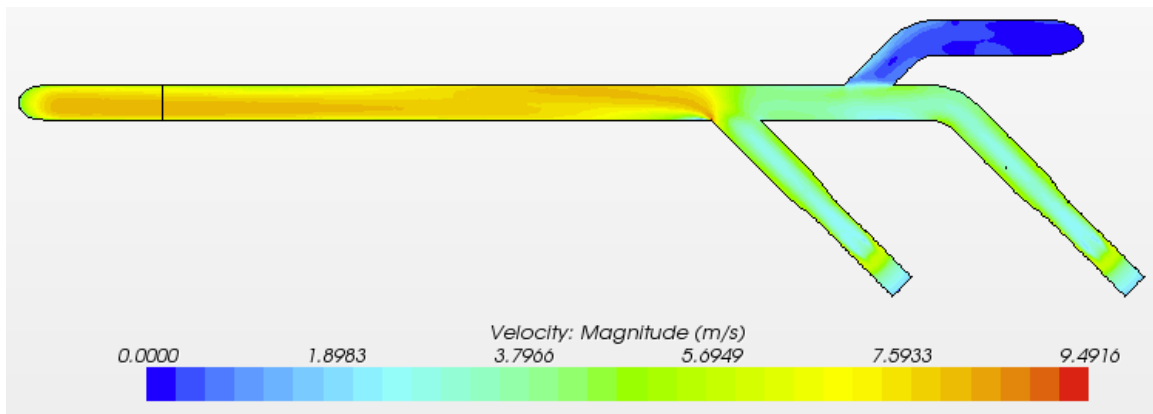


Figure 3.2. Velocity Magnitude in Plan View at Mid-Plane of the Main Duct for the Modeled VT-4 Flow Case

In testing, measurements are taken at the sampling section at 9 vertical and 9 horizontal locations across the duct. The COV is calculated as the quotient of the standard deviation and average value in the center 2/3 of the duct (7 of 9 locations), expressed as a percentage. In the present modeling work, predicted values from the same vertical and horizontal locations at the sampling section are used to calculate the COV.

The COV of velocity uniformity for tests VT-3 and VT-4, and the simulation cases representing them, are summarized in Table 3.1, where it is seen that the COVs from testing and from modeling are very similar. Table 3.2 summarizes flow angles from tests and the CFD simulations. The modeled flow angles are similar to angles measured in tests with similar flow rates (e.g., FA-2 and VT-3, FA-3 and VT-4). As demonstrated by the noise in the flow angle test data (Glissmeyer and Flaherty 2010), the flow distribution and flow angles are very dynamic, yet the flow angles predicted by the model compare well with the data. These results demonstrate the suitability of the model for simulating flow within the 3410 Building exhaust stack system.

Table 3.1. COV for Velocity Uniformity Tests VT-3 and VT-4

Test	Flow rate, acfm	COV from test, %			COV from model, %		
		Side	Top	All	Side	Top	All
VT-3	20,450	4.3	3.6	4.1	6.1	3.9	5.0
VT-4	12,351	2.4	3.7	3.4	7.0	3.6	5.4

Table 3.2. Maximum Flow Angles from Tests and Models

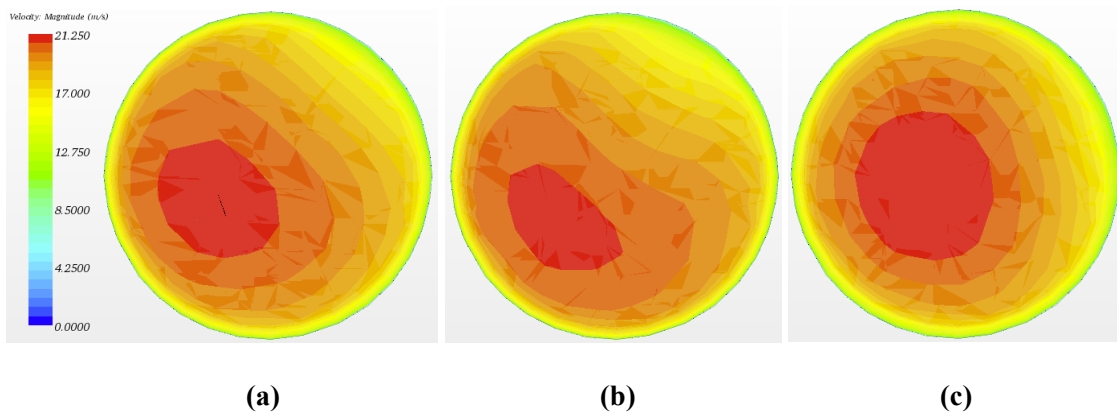
Case	Flow rate, cfm	Data source	Maximum flow angle	
			Side	Top
FA-1	17,975	measured	3.3°	11°
FA-2	18,350	measured	4.3°	5.7°
FA-3	10,800	measured	4.3°	5.7°
VT-3	20,450	modeled	5.4°	6.4°
VT-4	12,351	modeled	6.2°	5.2°

4.0 Stack Modeling Results

The 3410 Building filtered exhaust system, modified to include a third fan, is exercised in this section to examine the tracer gas mixing and tracer particle dispersion performance of the system operating at the design conditions. As such, the simulation cases include the three combinations of two fan operations with the third fan in standby. Section 4.1 presents the velocity uniformity and flow angle results showing compliance with the ANSI/HPS N13.1-1999 standard. Section 4.2 presents the tracer particle and tracer gas results for cases in which the tracers were released at the mid-duct location. Section 4.3 discusses tracer results for cases in which the tracers were released at the near-fan locations. Section 4.4 explores the addition of an air blender and the effect it has on the flow angle and velocity and tracer uniformity.

4.1 Flow Angle and Velocity Uniformity

Operations of the modified three-fan exhaust system will involve running two of the three fans at any given time, with one fan in reserve, for an expected maximum total flow rate of 31,840 cfm. Modeling cases were run to simulate the two-fan operations to determine the relative performance of each case and how well each case will meet ANSI standards. Figure 4.1 shows velocity magnitude distributions at the sampling section for the three two-fan operation cases. The color scales of the three contour plots match with flow velocities up to 21.25 m/s (3650 ft/min) mean. Due to a swirl component in the duct flow, the velocity profiles at the sampling/test section are skewed similarly to those of the VT-3 and VT-4 simulation cases. When operating fans 1 and 2 (Figure 4.1a) or 1 and 3 (Figure 4.1b), the velocity distributions are more skewed and less developed as when operating with fans 2 and 3 (Figure 4.1c). The flow is more developed in the latter case due to greater main duct length available with this fan combination. Although the distribution of velocity appears to be more uniform for the case running fans 2 and 3, all cases have similar velocity uniformity COV and maximum flow angles, as summarized in Table 4.1.



Note: Color scale: BLUE = 0 to RED = 21.25 m/s

Figure 4.1. Velocity Magnitude at the Sampling Section for the Modeled Flow Rate of 31,840 cfm, Running (a) Fans 1 and 2, (b) Fans 1 and 3, and (c) Fans 2 and 3

Table 4.1. COV for Velocity Uniformity and Maximum Flow Angles From CFD Modeling

Fans operating	Flow rate, cfm	Velocity uniformity COV, %			Maximum flow angle	
		Side	Top	All	Side	Top
1-2	31,840	5.7	4.4	4.9	5.8	6.7
1-3	31,840	4.0	6.6	5.4	7.3	7.0
2-3	31,840	7.2	4.0	5.6	6.8	7.5

4.2 Particle and Tracer Gas Distributions (mid-duct release location)

Particle and tracer gas transport simulations have been performed as a part of the 31,840 cfm, two fan cases. Particles are modeled as oil droplets of nominal 10-micron aerodynamic diameter, and the SF6 gas is modeled as a gas component in a mixture with the air stream. Tracer particles and tracer gas species are both introduced separately at the release location, just downstream of the confluence of the fan ducts (see mid-duct location in Figure 1.1).

Figure 4.2 shows the particle distributions at the sampling location for the two fan combination cases. The case running fans 1 and 2 (Figure 4.2a) has the greatest rotational flow component—due to the close proximity of fan 1—and the most particle dispersion at the sampling location. The case running fans 1 and 3 (Figure 4.2b) has less particle dispersion than with fans 1 and 2, apparently due to minimal swirl introduced by fan 3. The case running fans 2 and 3 (Figure 4.2c) has the least swirl and the least particle dispersion of the three cases. Figure 4.3 shows the tracer gas distributions at the sampling section for the two fan combination cases. The tracer gas distributions show similar spatial distributions as the particles. The case running fans 1 and 2 (Figure 4.3a) is the most mixed. The particle and tracer gas distributions presented in Figures 4.2 and 4.3 indicate that rotational flow, which is greatest when running fans 1 and 2, results in better particle dispersion and tracer gas mixing than when the rotational component of the flow is less.

COVs calculated from the distributions of particles and tracer gas are summarized in Table 4.2, where it is seen that in many instances the COVs are greater than the maximum acceptable COV of 20 percent across the sampling location. Thus, with the stack system operating on two fans at 31,840 cfm total flow, the modeling predicts that when injecting tracer gas and/or particles at the mid-duct location, the stack and sampling location will not be in compliance with the ANSI/HPS N13.1-1999 standard, with respect to particle distribution and tracer gas mixing.

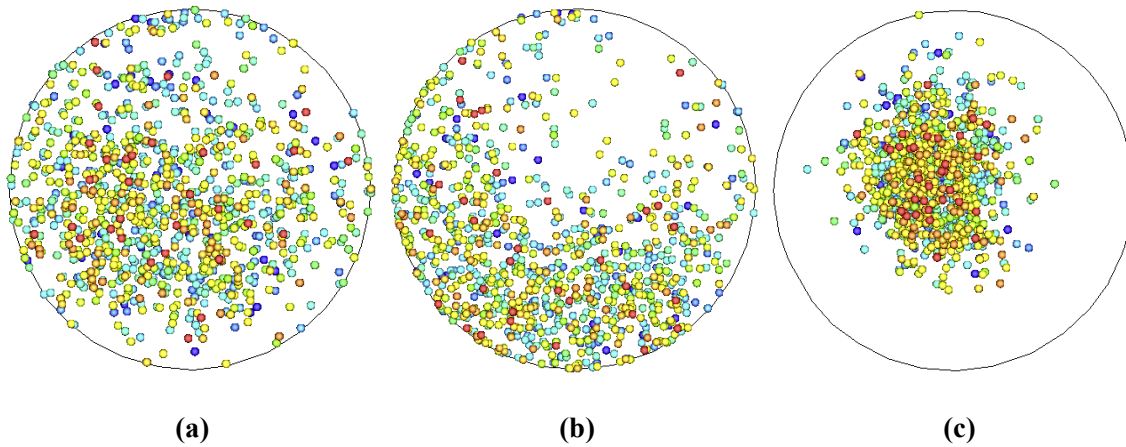
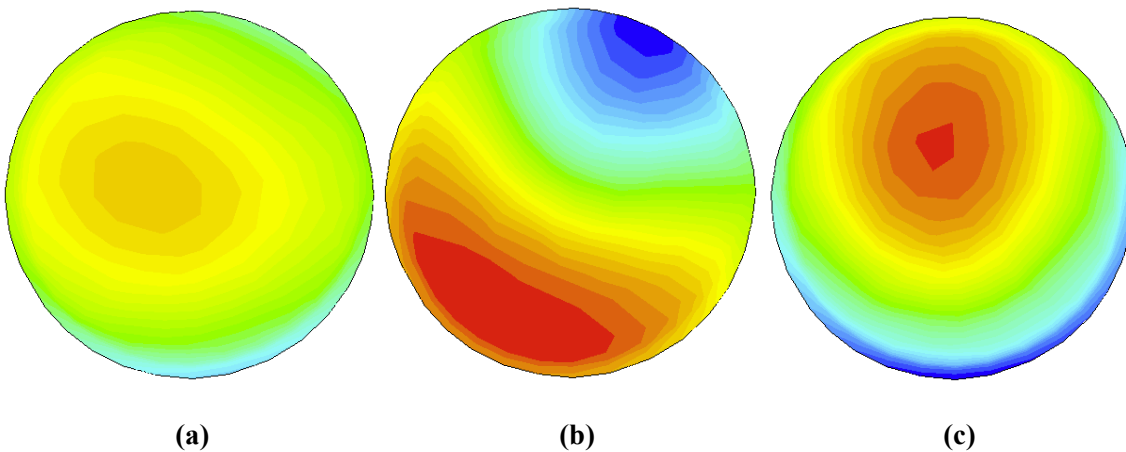


Figure 4.2. Particle Distributions at the Sampling Section for a Total Modeled Flow Rate of 31,840 cfm, Running (a) Fans 1 and 2, (b) Fans 1 and 3, and (c) Fans 2 and 3



Note: Highest concentration (red) is 2.7 times larger than lowest concentration (dark blue).

Figure 4.3. Tracer Gas Concentration Contours at the Sampling Section for a Total Modeled Flow Rate of 31,840 cfm, Running (a) Fans 1 and 2, (b) Fans 1 and 3, and (c) Fans 2 and 3

Table 4.2. COV for Particle and Tracer Gas Distributions at the Sampling Section

Fans operating	Flow rate, cfm	Particle COV, %			Tracer gas COV, %		
		Side	Top	All	Side	Top	All
1-2	31,840	35	39	36	5.0	7.2	6.2
1-3	31,840	64	28	50	15.1	30.7	24.0
2-3	31,840	62	54	58	11.6	14.5	12.8

4.3 Particle and Tracer Gas Distributions

Insufficient mixing and large COV values suggest the tracer release points would be best placed at locations that provide greater duct length for mixing of the tracers within the air streams. The maximum flow case (31,840 cfm) was rerun with tracer injection locations just downstream of the fans. This configuration gives greater duct length for mixing of the tracers than with the mid-duct release location. Three cases serve to examine the effect of using various tracer release locations. The cases included:

- Case 1: operating fans 1 and 2 with a tracer injection location near fan 1
- Case 2: operating fans 1 and 2 with tracer injection locations near both fans 1 and 2
- Case 3: operating fan 1 only (15,920 cfm) with a tracer injection location near fan 1.

The calculated COV results from these three cases are summarized in Table 4.3. With a single tracer injection point located near fan 1 (Case 1), the insufficient mixing seen with the mid-duct release location persists for both the tracer particles and tracer gas. Case 2, with injection locations near both fans, shows acceptable velocity, particle, and tracer gas uniformity COVs. These results indicate that mixing of the tracers within the stream of each fan is achieved and that blending of the two streams together in the main duct is more challenging. When running only fan 1 at full speed and injecting tracers near fan 1, as in Case 3, the velocity and tracer uniformity COVs within the single fan stream are similarly acceptable to those of Case 2.

These tracer release location simulation results are supported by the testing of Glissmeyer and Droppo (2007), which yielded tracer COV values greater than 20 percent at all but the test port furthest downstream, and showed that tracer gas and particle COVs were smaller when operating one fan than when operating two fans. However, as shown in Table 4.3, the overall velocity COV for Case 3 is the highest of the three cases. This is another result supported by the testing of Glissmeyer and Droppo, which showed that velocity uniformity was less for one-fan operations and improved for two-fan operations.

While the Case 2 simulation results show acceptable velocity, particle, and tracer gas COVs, the ANSI/HPS N13.1-1999 standard does not allow simultaneous injection of tracer gas/particles at multiple locations. Additionally, the particle COVs of the best cases presented here are marginally acceptable at best, indicating that additional blending would be desirable to ensure compliance.

Table 4.3. COV for Velocity, Particle, and Tracer Distributions at the Sampling Section

Case	Total Flow, cfm	Velocity COV, %			Particle COV, %			Tracer gas COV, %		
		Side	Top	All	Side	Top	All	Side	Top	All
1	31,840	5.4	4.4	4.7	32	51	29	15	39	29
2	31,840	5.4	4.4	4.7	19	17	16	2.5	4.6	4.1
3	15,920	8.6	2.4	6.3	20	18	18	3.4	6.0	5.0

4.4 Duct with Air Blender

The addition of an air blender in the main duct is being considered to ensure low COV values at the sampling location for all expected flow operations. The air blender being considered is from Blender Products, Inc¹. It is a static mixer of 40-inch diameter to match the diameter of the 3410 Building duct. Figure 4.4a is a photo of the device, and Figure 4.4b shows the CFD model of the device created for and used in the greater stack model that generated the results presented in this section. This section compares modeled results of the duct with total flow rate of 31,840 cfm, delivered by operating two fans, with and without the air blender.

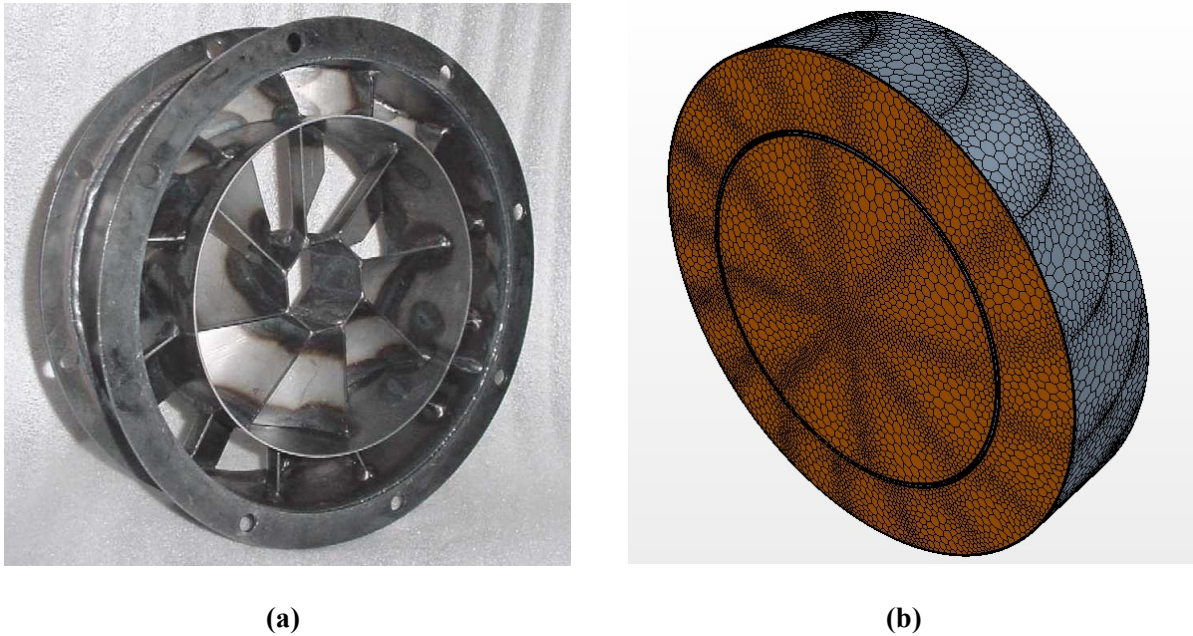
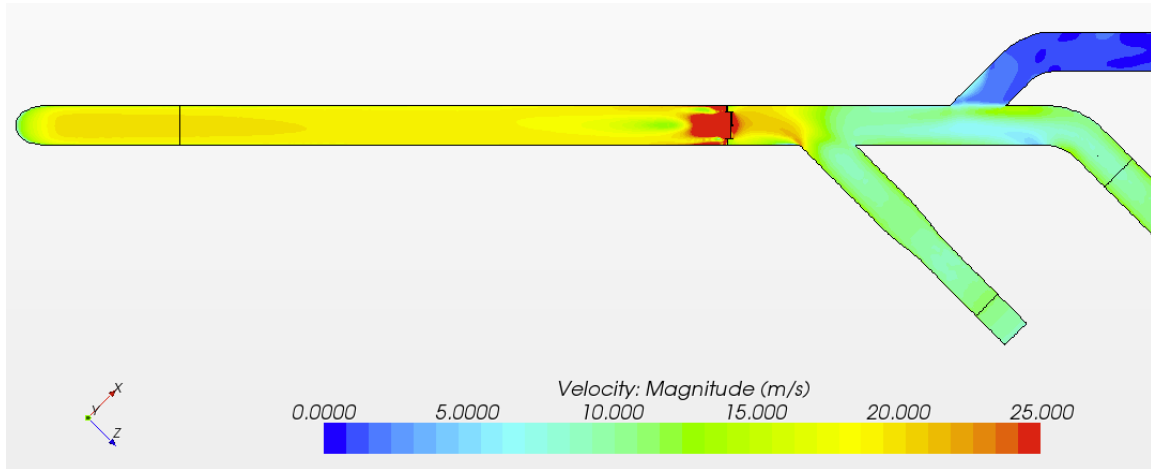


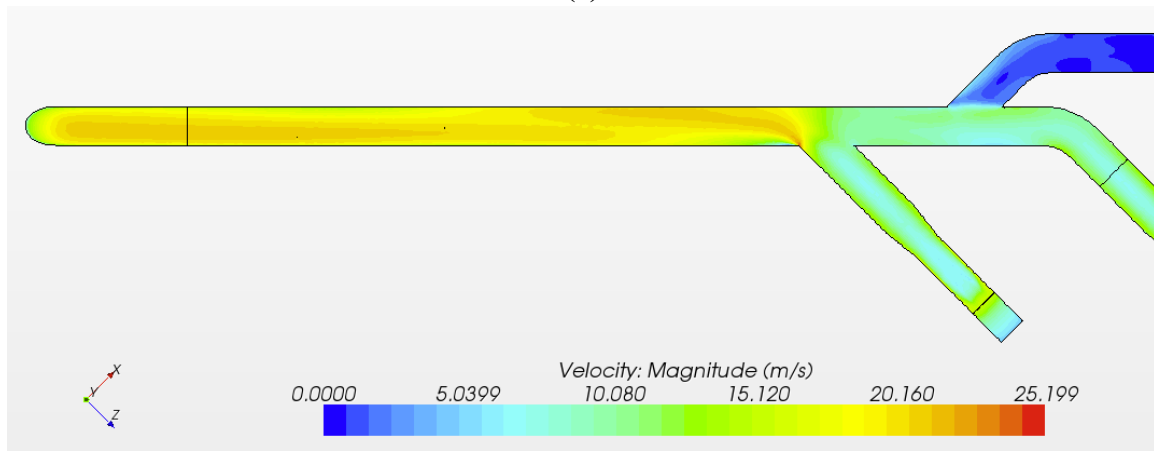
Figure 4.4. Static Air Blender S40C3S: (a) Photograph of Sample Device, (b) CFD Model

Figure 4.5 shows the effect of the air blender on the distribution of velocity magnitude within the 3410 Building stack with fans 1 and 2 operating. Figure 4.5a shows the contours of velocity magnitude in the plan view of the main duct with the air blender installed near the previous location of the mid-duct release point. Within a few duct diameters downstream of the blender, the velocity magnitude is symmetric across the duct and roughly uniform. Figure 4.5b shows the contours of velocity magnitude without the air blender. In this latter case, the flow swirls slowly downstream and is non-symmetric and non-uniform at the test section.

¹ Blender Products Inc. 5010 Cook Street, Denver, CO. 80216 [phone: 800-523-5705]



(a)



(b)

Figure 4.5. Contours of Velocity Magnitude in the Plan View for (a) the Duct with the Air Blender Installed, and (b) No Air Blender

Figure 4.6 shows the effect of the air blender on the distribution of SF₆ tracer gas within the 3410 Building stack system. As with the velocity magnitude, the tracer gas concentration is symmetric across the duct and roughly uniform within a few duct diameters downstream of the blender, as shown in Figure 4.6a. Without the air blender, the tracer gas follows the air flow pattern and is non-symmetric and non-uniform at the test section (Figure 4.6b).

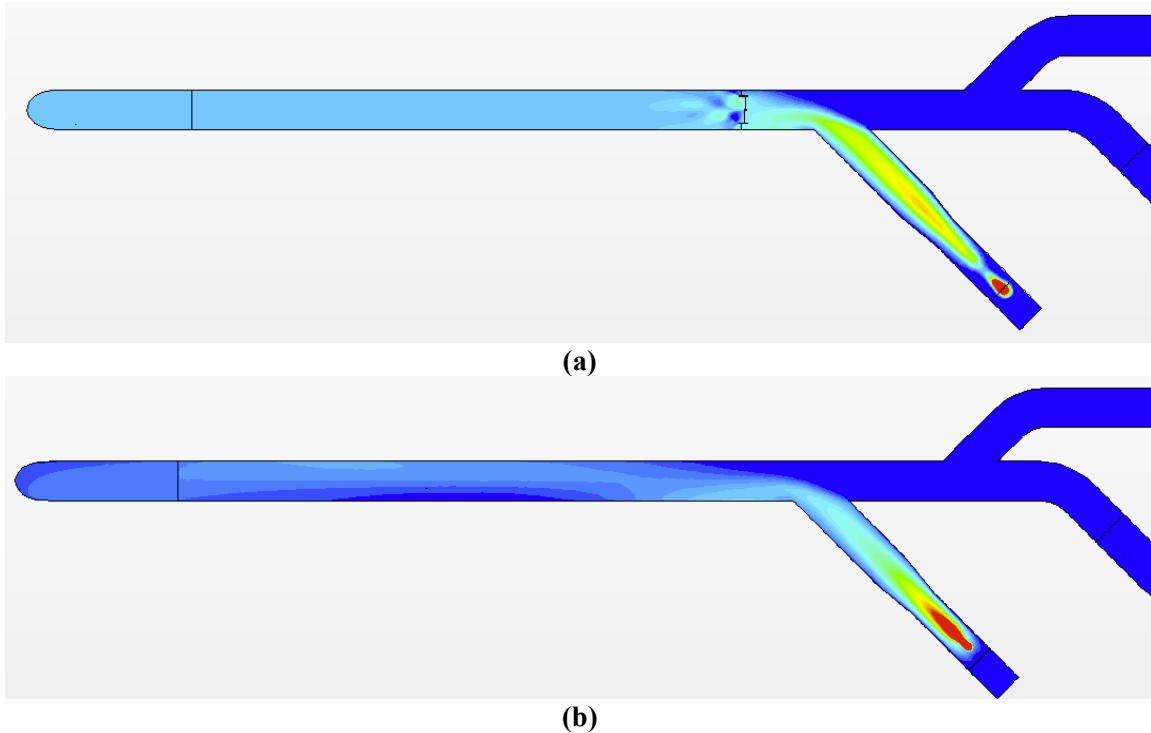
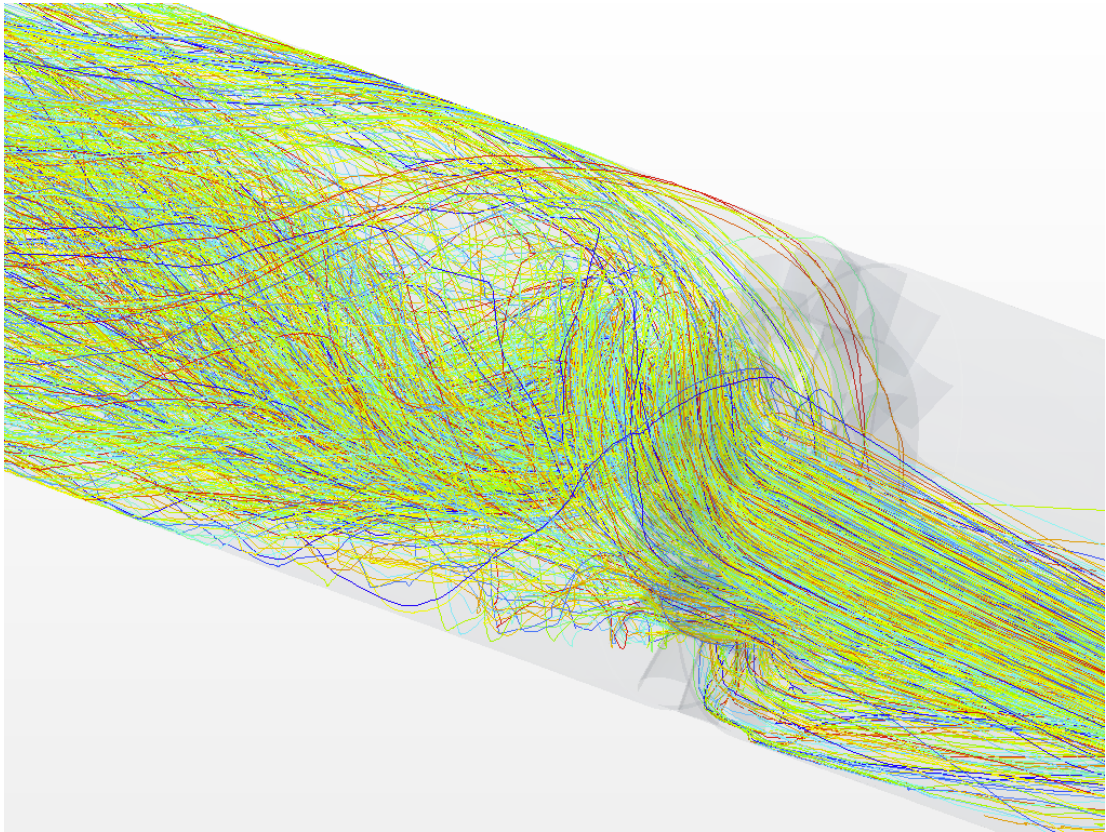
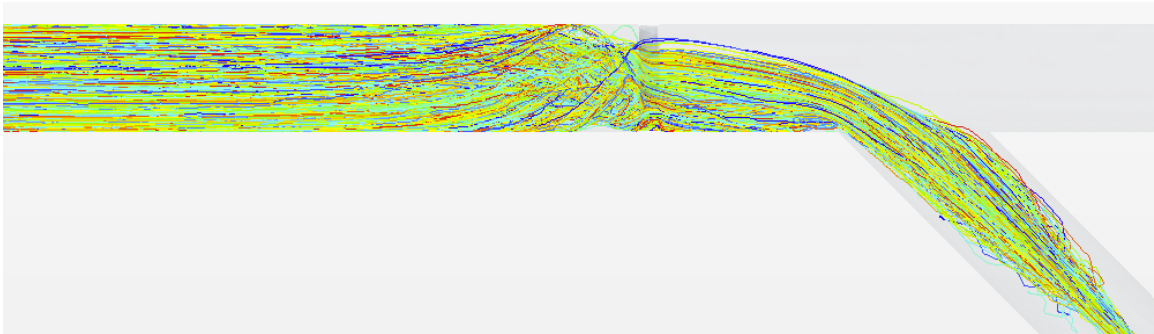


Figure 4.6. Contours of SF6 Tracer Gas Concentration in Plan View for the Duct with (a) the Air Blender Installed, and (b) No Air Blender

The counter-rotating inner and outer flows through the air blender serve to mix the air within just a few duct diameters, downstream of which the flow settles into a non-circulating pattern. This effect can be seen in Figure 4.7a, which shows tracer particle paths through the air blender being quickly dispersed downstream of the device. Figure 4.7b shows the same particle paths in plan view. In this expanded view, the particle paths within about 3 to 5 duct diameters have been dispersed and are traveling straight down the duct. The particle dispersion is illustrated by Figure 4.8, which shows particle distributions at several stations downstream of the air blender. At 1 duct diameter, the particles are somewhat scattered, but by 5 diameters the particles are well dispersed. Likewise, at 10 diameters and at 14 diameters, where the sampling section is located, the particles are well dispersed within the duct.



(a)



(b)

Figure 4.7. Tracer Particle Paths Through the Air Blender: (a) 3-D View, and (b) Plan View

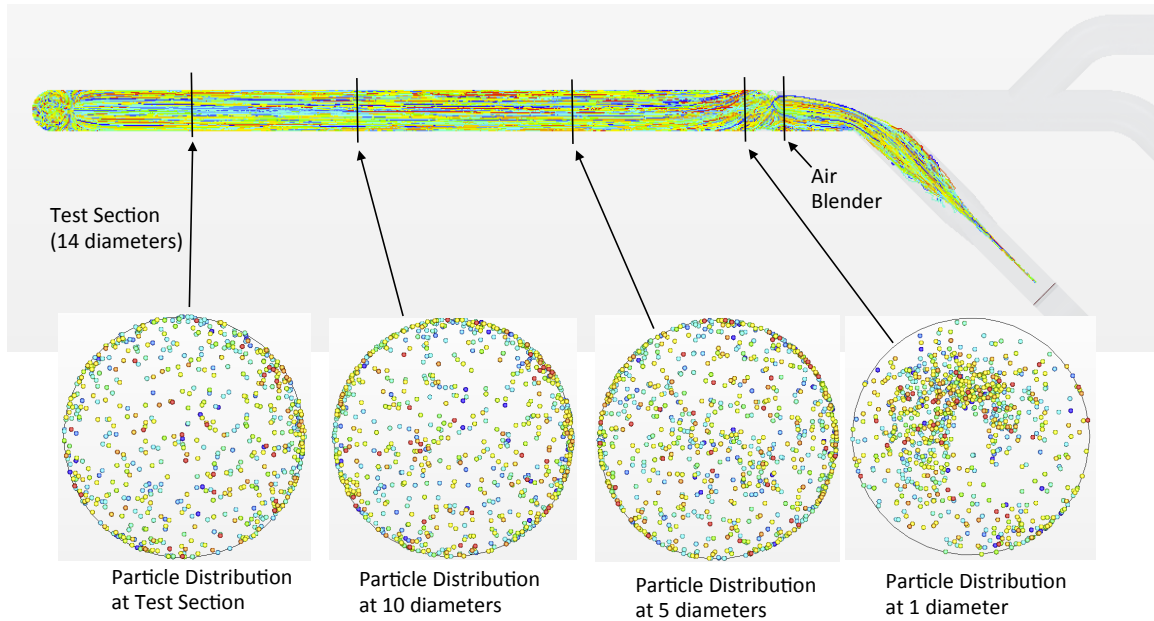


Figure 4.8. Tracer Particle Distributions at Several Stations Downstream of the Air Blender

Maximum flow angles and velocity, tracer gas, and tracer particle COVs at various stations downstream of the air blender inlet are shown in Figure 4.9. The maximum flow angle at 1 duct diameter downstream of the air blender is quite large at 43 degrees; the angle then decreases to about 1 degree at 5 diameters and is less than 1 degree at greater distances downstream. Similarly, tracer gas and velocity COVs decrease to quite small values within 5 diameters downstream of the air blender. COVs for the tracer particles are also well within compliance values. These results indicate that the addition of the Blender Products, Inc. air blender to the 3410 Building filtered exhaust stack system will ensure compliance with the ANSI/HPS N13.1-1999 standard.

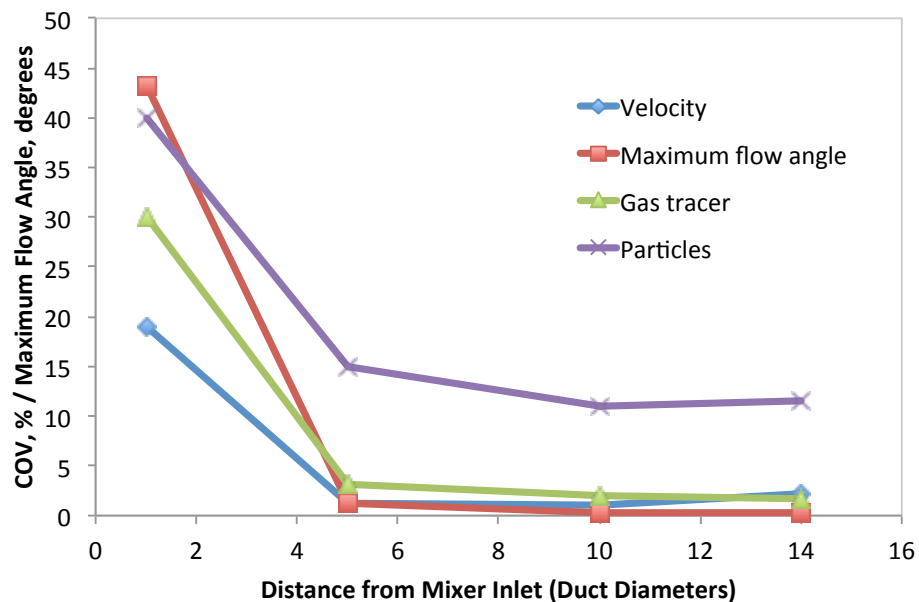


Figure 4.9. Maximum Flow Angle (degrees) and COV for Velocity, Tracer Gas, and Tracer Particles with Air Blender

5.0 Conclusions

Based on the CFD modeling of the 3410 Building filtered exhaust stack system, the following conclusions are drawn:

- The CFD model provides flow angle and velocity uniformity COV values that are in good agreement with those derived from testing of the original stack configuration with two fans, operating at approximately 20,000 cfm.
- Modeling results for the new configuration running two of three fans and operating at a maximum total flow of 31,840 cfm predict that differences in the flow distributions at the sampling location will exist depending upon the fan combination used, but that the velocity uniformity COV values should remain well within compliance.
- Simulations of tracer gas mixing and tracer particle dispersion within the duct show that tracer release points are best placed at locations that provide greater duct length for mixing of the tracers within the air streams.
- Simulations examining the effect of using various tracer release locations show that mixing of tracers within the stream of each fan is achieved much more readily than blending of the two fans streams together in the main duct. These simulations also show that tracer COV values are smaller when operating one fan than when operating two fans, yet the velocity COV is greater for one fan than for two. These results are supported by experimental data.
- Modeling results of the duct with total flow rate of 31,840 cfm delivered by two-fan operations predict that velocity uniformity, tracer concentrations, and flow angle criteria established by the ANSI/HPS N13.1-1999 standard will be met with the addition of the Blender Products, Inc. air blender.

6.0 References

ANSI/HPS N13.1-1999. 1999. *Sampling and Monitoring Releases of Airborne Radioactive Substances from the Stack and Ducts of Nuclear Facilities*. American National Standards Institute/Health Physics Society, McLean, Virginia.

CD-Adapco. 2012. User Guide STAR-CCM+ 7.02.011.

Incropera FP and DP DeWitt. 1985. *Introduction to Heat Transfer*, second edition. John Wiley and Sons, New York.

Jensen BBB. 2007. “Numerical Study of Influence of Inlet Turbulence Parameters on Turbulence Intensity in the Flow Domain: Incompressible Flow in Pipe System.” *Proceedings of the Institution of Mechanical Engineers, Part E: Journal of Process Mechanical Engineering* 221(4):177-186.

PNNL-16611. 2007. *Assessment of the HV-C2 Stack Sampling Probe Location*. JA Glissmeyer and JG Droppo, Pacific Northwest National Laboratory, Richland, Washington.

PNNL-19562. 2010. *Assessment of the 3410 Building Filtered Exhaust Stack Sampling Probe Location*. JA Glissmeyer and JE Flaherty, RPT-STMON-005, Pacific Northwest National Laboratory, Richland, Washington.

Recknagle KP, ST Yokuda, MY Ballinger, and JM Barnett. 2009. “Scaled Tests and Modeling of Effluent Stack Sampling Location Mixing.” *Health Physics* 96(2):164-174.

Young DF, Munson BR, and Okiishi TH. 1997. *A Brief Introduction to Fluid Mechanics*. John Wiley and Sons, New York.



Pacific Northwest
NATIONAL LABORATORY

*Proudly Operated by **Battelle** Since 1965*

902 Battelle Boulevard
P.O. Box 999
Richland, WA 99352
1-888-375-PNNL (7665)
www.pnnl.gov



U.S. DEPARTMENT OF
ENERGY